Polymer Journal, Vol. 36, No. 9, pp. 684—694 (2004)

^{1}H Spin–Spin Relaxation Time of Water and Rheological Properties of Cellulose Nanofiber Dispersion, Transparent Cellulose Hydrogel (TCG)

Hirofumi ONO,† Yoshihiko SHIMAYA, Kazuishi SATO, and Tomoko HONGO

Central Research Laboratory, Asahi Kasei Corporation, 2-1 Samejima, Fuji 416-8501, Japan

(Received December 11, 2003; Accepted May 19, 2004; Published September 15, 2004)

ABSTRACT: A new type of hydrogel, transparent cellulose hydrogel (TCG), is the aqueous dispersion of cellulose nanofibers (microfibrils) 10 nm in width and several hundreds nanometers in extended fiber length, and shows unique rheological properties leading to unique applications. The rheological properties of TCG, especially their dependences on temperature were investigated through the spin–spin relaxation time (T_2) analysis in ^{1}H NMR for water in the systems. Viscosity under low shear stress and T_2 of water (being very short for T_2 value) were proved to be constant in a wide range of temperature (*ca.* 30–80 °C). These results may be explained by two considerations that network in TCG gradually grows with increasing temperature but collapses by adding weak shear stress and that TCG gel has large amount of bound water. It was also confirmed that the ionic strength such as pH and NaCl concentration sensitively influences on rheological parameters. With increasing ionic strength, the network formation and the successive aggregation of microfibrils occur and both should be interpreted in terms of the electrostatic interaction between negative charge on a cellulose surface and cationic aqueous layer around it (*i.e.*, electric double layer).
[DOI 10.1295/polymj.36.684]

KEY WORDS Cellulose / Hydrogel / Nanofiber / Microfibril / Rheology / Spin–Spin Relaxation Time / Network /

We have already found a preparation method of a new type of hydrogel, transparent cellulose hydrogel (TCG, Figure 1a), an aqueous dispersion of cellulose microfibrils (degree of polymerization: *ca.* 40) having low crystallinity with about 10–15 nm in diameter and several hundred nanometers in extended length (Figure 1b) and reported the results for its characterization and properties.[1,2]

This new nanomaterial was prepared by downsizing by chemical (hydrolysis reaction)[3] and mechanical (smashing by a ultra high pressure homogenizer) techniques. Resultant cellulose microfibrils in TCG are flexible fibrous particles, *i.e.*, "nanofibers", having nano-size diameter (Figure 1b) and show strong attractive interaction based on hydrogen bonding between hydroxyl groups localized densely on their surfaces, leading to quite unique rheological properties.[2]

In view of the application, four major unique properties of TCG are pointed out[2] as follows:
1) Rheological properties such as very high viscosity under the low share stress, a large thixotropic character and low fluctuation of rheological parameters in the range of ambient temperature to the higher temperature region, 2) Formation of transparent coating film on substrate materials by drying, 3) Formation of cellulose microspheres having average particle size of less than 5 μm by spray drying, and 4) Stabilizing ability as an additive for aqueous suspension systems such as aqueous dispersion of inorganic particles (SiO_2, TiO_2, …, etc.) and O/W type emulsion (also as an emulsifier).

Especially from an industrially applicable aspect, we discovered that TCG is a gel which can be sprayed by only using a conventional spraying apparatus under an atmospheric pressure.[4] This unique utility for TCG closely is related to the above rheological characteristics.

Ono *et al.* revealed[5] that ^{1}H NMR relaxation (spin–spin relaxation time, T_2) analysis for water[6,7] is effective to elucidate the relationship between viscosity and dispersion state of particles in aqueous suspension of microcrystalline cellulose (MCC) having a rod-like figure with several micrometers in longitudinal length.[3,5,8] They concluded that T_2 of water critically reflects the relatively mild aggregation (association) state of MCC in the suspension. In the case of MCC suspension, the dispersion state of MCC could be observed directly by an optical microscope owing to relatively large size. This method, however, could not be applied to TCG because of the smaller particle size. Therefore, we believe that T_2 analysis on water in TCG or its diluted dispersion is effective to elucidate why such properties as above appear in the systems.

The nature of this hydrophilic colloid, TCG, should be understood through knowledge of network formation in aqueous media as function of attractive (hydro-

†To whom correspondence should be addressed (E-mail: ono.hp@om.asahi-kasei.co.jp).

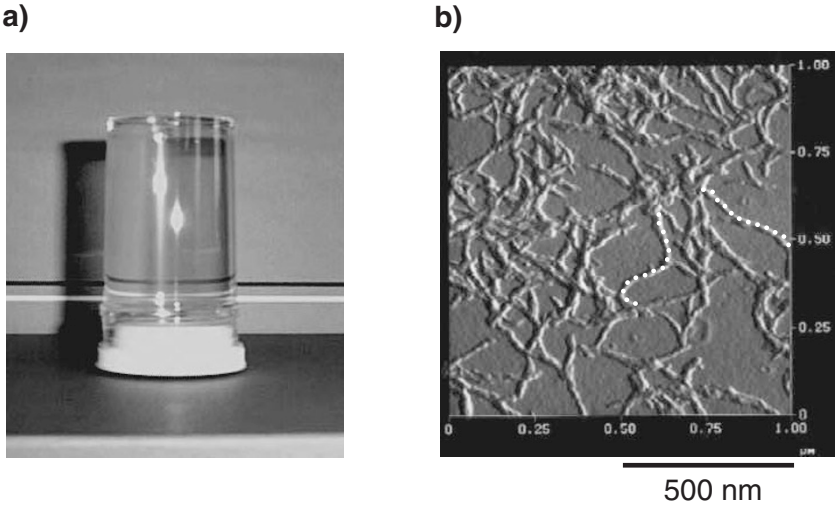

Figure 1. (a) TCG-2.0 sample. Sample has high transparency and gel-like high viscosity where the content does not flow even turning the sample tube upside down. (b) AFM images of as-cast residue on a glass plate cast from highly diluted suspension of TCG-2.0 after ultrasonic treatment. The dotted line shows an image of single microfibril.

gen bonding) and repulsive (electrostatic repulsion) forces. As shown in the previous report,[2] the surface of the microfibrils constituting TCG has a slightly negative ζ potential (*ca.* -30 mV) in neutral pH region as in the case of the other typical celluloses.[9] According to Derjagumi–Landau–Verway–Overbeek (DLVO) theory[10,11] the electrostatically charged particles in aqueous medium form so-called electric double layer on their surfaces, giving reverse electrical charge to the outer layer (that is, surrounding surface). The total network structure in TCG might be determined by the balance of attractive force (hydrogen bonding) and an electrostatic repulsion working on the surface.

This paper correlates rheological properties of TCG to the dispersion state of nanofibers (cellulose microfibrils) in aqueous medium by T_2 analysis of water by using a pulse NMR spectrometer. For this purpose, we especially focused on the rheology as a function of temperature and ionic strength.

EXPERIMENTAL

Sample Preparation

TCG samples were prepared according to the procedure described in the previous paper[2] as follows: The dissolving pulp (as a purified cellulose) was dissolved into the 65 wt % sulfuric acid at 0 °C. The solution was poured into water (water/solution ratio = 2.29 (g/g)) to precipitate regenerated cellulose in flock state with 5–10 mm in size. The cellulose suspension was heated to 80 °C and kept at this temperature for 20 min (hydrolysis processs). The suspension after the heat treatment was filtrated on a glass filter and washed with large amount of water repeatedly. A white and translucent cake composed of cellulose (6 wt %) and water (94 wt %) in nearly neutral pH was obtained (pre-TCG).

Pre-TCG was diluted by water so as to make 1.5 wt % to 4 wt % cellulose suspension, then pre-mixing was carried out by using a homomixer, T.K.Robo mics™ (Tokusyu Kika Kogyo Co., Ltd., Japan). Each dilute dispersion of pre-TCG was smashed into finer fragments by passing through a ultra high pressure homogenizer, Microfluidizer™ M-110EH (Mizuho Kogyo Co., Ltd., Japan). The smashing conditions were as follows: operating pressure: 175 MPa, a passing times: five times. In all cases, transparent and gel-like TCG samples were obtained. Hereafter, TCG sample obtained from the diluted pre-TCG dispersion in which cellulose concentration was adjusted to *x* wt % referred to as TCG-*x* (*e.g.*, TCG-4.0).

pH and ionic strength of TCG were controlled by adding either HCl or NaOH, and NaCl, respectively. TCG with no specification of pH is a neutral sample (pH = 6.0–6.5).

Measurements of Viscosity

Viscosity (η) *vs.* shear rate ($\dot{\gamma}$) relationship and η *vs.* shear stress (σ) relationship were measured at controlled shear rate using a rotation type viscometer (Rheo Stress, RS100, Haake Co., Ltd., Germany) with either cone-plate (cone angle: 4°, diameter of the plate: 35 mm) or double cylinder equipment (content: 9 mL) at 25 °C. The temperature dependence of viscosity was measured by a B-type viscometer (model BH, Tokimec INC, Japan) at four rotation rates (2, 5, 10 and 20 rpm) and the temperature of TCG stocked in a 500 mL beaker was controlled by a water bath.

Measurements of T_2

T_2 of water in TCG was measured according to Carr–Purcell–Meiboom–Gill (CPMG) method[12] by using a pulse NMR spectrometer (JNM-Mu25; JOEL Co., Ltd., Japan). TCG sample was set in a sample tube (diameter: 10 mm, height of injected sample: *ca.* 10 mm) and enclosed. Each relaxation curve is described by a simple exponential;

$$M_t = M_0 \exp\left(-\frac{t}{T_2}\right) \quad (1)$$

Here, M_0 is an initial magnetization, and M_t is the magnetization at time t.

RESULTS AND DISCUSSION

Rheological Properties of TCG

Figure 2a and b shows the relationships between viscosity (η) and shear rate ($\dot{\gamma}$), and between η and shear stress (σ) measured at 25 °C for TCG-1.5, respectively. The results for two conventional hydrogel samples (aqueous gels of partially crosslinked acrylic copolymer, Carbopol-940™ (CP-940, Chugai Boyeki Co., Ltd., Japan) and polyacrylamide (PAcAm, Tokyo Kasei Kogyo Co., Ltd., Japan)) and typical aqueous polymer solution (aqueous solution of hydroxy-ethylcellulose (HEC, Tokyo Kasei Kogyo Co., Ltd., Japan)) are shown for comparison. Here, the polymer content of all samples was adjusted to 1.5 wt %.

In Figure 2a, the η *vs.* $\dot{\gamma}$ curve for HEC solution shows very little $\dot{\gamma}$ dependence of viscosity as found in a typical polymer solution having a low thixotropic nature.[13] In contrast, that for TCG-1.5 shows drastic decrease of viscosity from 10^7 mPa s to 10^2 mPa s with increasing $\dot{\gamma}$. This means that TCG is a typical thixotropic material like the case of the hydrogel samples of CP-940 and PAcAm. An aqueous suspension of MCC similarly is highly thixotropic.[5] TCG-1.5 should have very large zero-shear viscosity scince the peak top value (η_{max}) on the η *vs.* $\dot{\gamma}$ plot can be regarded as an approximate value of a viscosity under zero-shear condition.

In Figure 2b, η *vs.* σ relationships of three hydrogel samples show clear yield points denoting the collapses of network structures under a certain stress. TCG has a relatively low yield point for high η_{max} (compare the profile of TCG-1.5 with that of CP-940 hydrogel). This probably originates from the fact that TCG is "colloidal gel" in which the crosslinking point in network is based on the surface–surface attractive interaction between microfibrils. In contrast, the network in the conventional hydrogel is composed of polymer chains and therefore the network density is much larger than that for TCG. Thus, the crosslinking density of TCG is overwhelmingly lower than that of the other

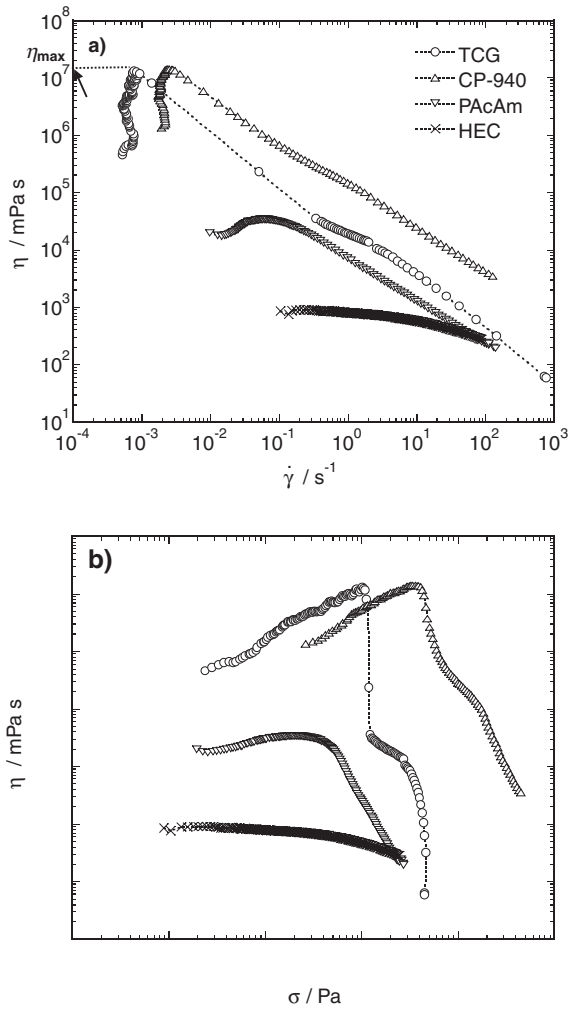

Figure 2. Shear rate $\dot{\gamma}$ (a) and shear stress σ (b) dependence of the viscosity, η estimated at 25 °C for four samples, TCG-1.5, the aqueous gel of partially crosslinked acrylic copolymer, Carbopol-940™ (CP-940), the aqueous gel of polyacrylamide (PAcAm) and aqueous solution of hydroxyethylcellulose (HEC). The polymer content of all samples was adjusted to 1.5 wt %.

conventional hydrogels, resulting in smaller yield points. This property might be important, particularly in application, because TCG easily changes to liquid-like dispersion only by adding relatively low shear stress. Thus, the unique rheological properties of TCG are significantly related to the network structure comprised of cellulose microfibrils in aqueous media.

Figure 3a gives the SEM micrograph of the freeze-dried sample of TCG-2.0, regarded as a model of network structure in TCG-2.0. By adding a certain shear stress on TCG-2.0, the network easily collapses to the dispersion of microgels composed of the microfibril associates depending on the magnitude of added stress (Figure 3b). The viscosity of TCG is determined by a dispersion state of microfibrils. If a sufficiently large shear stress (or dispersing power, *e.g.*, the use of Microfluidizer™) is added on TCG gel, the gel changes

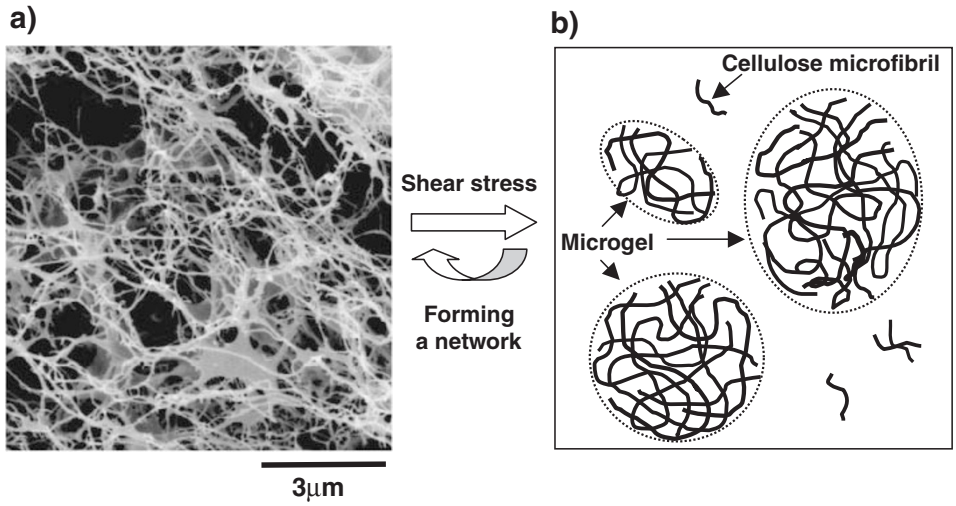

Figure 3. Models of the network structure of TCG (a) and dispersing state after collapsing of network by a certain shear stress (b) (a: SEM micrograph of the freeze-dried sample of TCG-2.0).

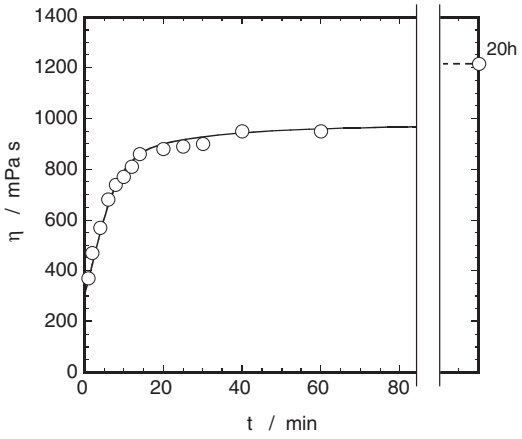

Figure 4. Standing time (t) dependence of the viscosity of TCG-2.0 at a rotating rate of 2 rpm, measured by B-type viscometer at 20 °C on standing immediately after mixing by a Warning Blender™ for one minute.

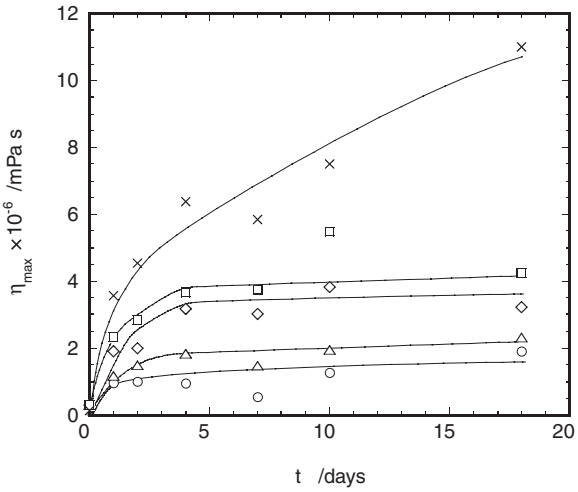

Figure 5. Standing time (t) dependence of η_{max} in the long interval at various standing temperatures for TCG-1.5-T0 (○; 4 °C, △; 20 °C, ◇; 40 °C, □; 60 °C) and TCG-1.5-M0 (×; 40 °C): TCG-1.5-T0 was prepared by diluting TCG-4.0 to give cellulose content of 1.5 wt % by dispersion using a T.K.Lobo.mics™ (10000 rpm × 20 min). TCG-1.5-M0 was prepared by diluting TCG-4.0 to give cellulose content of 1.5 wt % by dispersion using a Microfluidizer™ (passing time: one, pressure: 50 MPa).

to fluidic suspension like as a dispersion of individual microfibrils. Much lower viscosity is obviously due to a perfect collapse of network. However, the reconstruction of the network is started in local area immediately after the removal of the shear stress and gradually spreads out to a larger area by an association. The viscosity might become larger with growth of local network.

Figure 4 indicates the reserving time dependence of viscosity measured at a rotation rate of 2 rpm by a B-type viscometer at 20 °C, for the TCG-2.0 sample on standing immediately after mixing by Warning Blender™ for 1 min. More than 70% of the viscosity recovery was accomplished in the first 20 min. The viscosity gradually approaches the asymptotic value, *e.g.*, after 20 h.

The viscosity of TCG strongly reflects the dispersion state of microfibrils and is sensitively influenced by a shear stress history.

Influence of Temperature on the Rheological Properties of TCG

Figure 5 shows the recovery of viscosity (η_{max}) for TCG-1.5-T0 and TCG-1.5-M0 on standing at different reserving temperatures (4–60 °C) immediately after dispersion. These two samples were prepared by diluting TCG-4.0 with deionized water 1.5 wt % in cellulose content and then dispersed by two different methods. Suffixes T0 and M0 mean that the samples are

dispersed at 10000 rpm for 20 min by a homomixer (T.K.Lobo.mics™) and dispersed by passing the sample under 50 MPa through Microfluidizer™. TCG-1.5-M0 is considered to consist of the smaller microfibril associates (microgel) than TCG-1.5-T0. The network formed in TCG collapses to fragments (microgels or microfibrils) with very small size immediately after dispersion treatment and the restructuring of network occurs depending on a reserving temperature.

In the case of TCG-1.5-T0, increasing rate of viscosity and asymptotic (equilibrium) viscosity η_e became higher with increase in reserving temperature. This is explained as follows; The motion of individual microfibrils and their associates (microgel) in the treated TCG dispersion might be greatly influenced by the molecular motion of the media (water), being more enhanced for a higher temperature. The molecular motion of water facilitates the occurrence of mutual collision of microfibrils (or their associates), leading to the growth of the microgel, followed by formation of the higher ordered and equilibrium network. A higher ordered network structure might be preferably formed at a higher temperature owing to the above reason.

In the case of TCG-1.5-M0 at 40 °C, since the restructuring of network starts from a smaller-size structural units (in other words, a larger number of starting units), more time is required for recovering viscosity than for the TCG-1.5-T0 sample. A comparison with the results at 40 °C indicates that the recovering of η_{max} for TCG-1.5-M0 is much higher than that of TCG-1.5-T0. η_{max} of TCG-1.5-M0 does not reach to plateau even after 18 d. The reason for this may be that the dispersion state produced by using a ultra high pressure-homogenizer (TCG-1.5-M0) gives more suitable starting environment for the construction of the microfibril network than that by using a conventional homomixer (TCG-1.5-T0). In other words, a more ideal network may be constructed in the case starting from the more finely dispersed local networks (or individual microfibrils) because the degree of freedom in network formation is higher in such case. This speculation will become clearer with the model shown in Figure 3, and is very important to comprehend the rheological properties of TCG.

Figure 6a and b shows the relationship between viscosity and rotation rate at different temperatures, and the relationship between viscosity and temperature at two rotation rates. A B-type viscometer was used to cover a wider temperature region. For comparison, data for the aqueous solution of hydroxyethyl cellulose (HEC; Tokyo Kasei Co., Ltd.) are also shown.

The viscosity of HEC solution is almost independent of rotation rate as shown in Figure 2a. In contrast, the viscosity of TCG decreases considerably with increasing rotation rate, owing to its thixotropic nature as described already and was confirmed to be higher at higher temperatures, meaning that a higher-ordered network is formed at a higher temperature. The viscosity of HEC both at 2 and 20 rpm decreases almost linearly with increasing temperature. Incontrast, for TCG, the viscosity at 2 rpm shows no dependence on temperature, but that at 20 rpm decreases with increasing temperature like the case of HEC solution. This is explained by the viscosity–shear stress relation shown in Figure 2b. The network structure of TCG is quite stable at low shear stress region and resists the increased thermal motion of water molecules at higher temperatures. Here, the backbone of network is composed of nanofibers, which are larger than water molecules. However, network in TCG almost collapses at 20 rpm which corresponds to high shear stress region

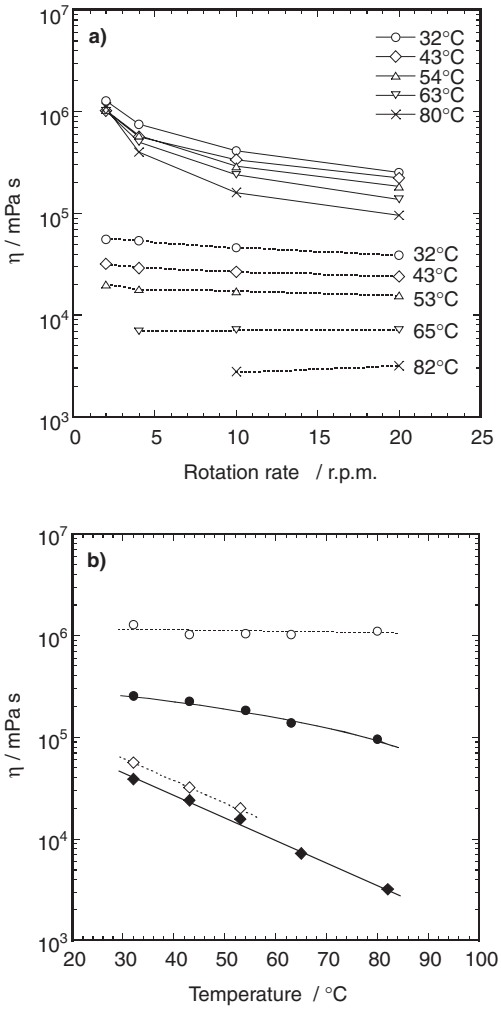

Figure 6. (a) Relationship between viscosity (η) and rotating rate measured by a B-type viscometer for TCG-2.0 and 2.0 wt % aqueous HEC solution (broken line; HEC. Solid line; TCG-2.0) at different temperatures, (b) Temperature dependence of viscosity (η) of TCG-2.0 and 2 wt % aqueous HEC solution at rotation rates of 2 rpm (open mark) and 20 rpm (closed mark). (○, ●; TCG, ◇, ◆; HEC sol.)

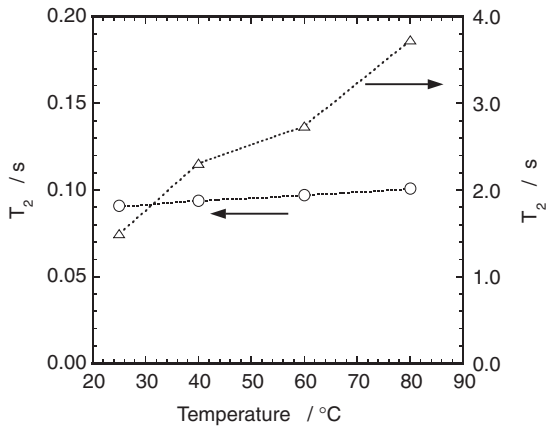

Figure 7. Temperature dependence of T_2 of water in TCG-2.0 and 2 wt % aqueous HEC solution. (○, TCG-2.0, △, HEC sol.)

in Figure 2b, so that cellulose microgels are dispersed in the aqueous phase. Under such high shear stress, the association between microgels is restricted, and the motion of microgels could be more influenced by the increased thermal motion of water at a higher temperature.

To confirm the above consideration, ^{1}H T_2 of water in TCG was measured as a direct index of water motion. Figure 7 shows the relationship between T_2 and temperature for TCG-2.0 and 2 wt % HEC solution. This figure shows large differenece in magnitude of T_2 for two samples. T_2 (1.9 s) of HEC at 25 °C is slightly shorter than that of deionized water (3.0 s at 25 °C), but TCG shows a drastically shorter T_2 (0.073 s).

In the case of a water-rich system such as aqueous suspension or aqueous solution, only one ^{1}H T_2 component is detected in CPMG measurement using a pulse NMR spectrometer.[5] This is explained by averaging of T_2 based on the faster exchange of water molecules between the phases of free water and bound water in comparison with a time scale (~100 ms) of NMR.[5,15] The very short T_2 for TCG is due to the contribution of the water strongly interacting with surface of cellulose particles ("bound water"). In the previous work[5] for aqueous MCC suspension, T_2 of water at 25 °C in 2 wt % MCC/water suspension was 0.21–0.22 s, about twice the present TCG. This suggests that the contribution of bound water is larger for TCG than for MCC suspension. In the case of HEC solution, HEC chains molecularly dispersed (dissolved) in water may cooperatively move with surrounding water molecules. Consequently even water molecules interacting strongly to a HEC chain are considered to be in the more dynamic (or more rapidly exchanging) environment compared with water around microfibril surface. Such dynamic property of bound water around HEC chains may cause T_2 of water in HEC solution to become much longer than that in TCG.

T_2 generally becomes longer with increasing temperature because of more active motion at higher temperatures.[14] This for water in HEC, but T_2 of water in TCG showed very small temperature dependence.

An assuming that 98 wt % of water in TCG-2.0 consists of free water and bound water and that observed T_2 is determined by averaging of T_2 for free water and bound water, the observed T_2 is strongly affected by both T_2 values and their fraction.[15] The reason for the small temperature dependence of T_2 observed for TCG can be explained by the models in Figure 8.

In the model, the amount of bound water increases with increasing temperature and intimately relates to the network formation in TCG. As described already, network in TCG grows more effectively at higher temperatures probably owing to higher frequency of collision between microfibrils. Figure 8a shows dispersion in TCG at a low temperature where independent microfibrils are dispersed in water. In such state, bound water is on an individual microfibril surface. Figure 8b shows the model at a relatively high temperature. Multiple microfibrils loosely associate each other to form a local network. By forming a new network domain, the enclosed space surrounded by some microfibrils (*e.g.*, the area surrounded by a dotted line in Figure 8b) is probably formed and is filled with new bound water by what we call "capillary effect".[5,16] Since bound water in such enclosed space is not perfectly sealed by microfibril walls and is linked continuously with bound water on the microfibril surface, an exchange of water between the free water phase and bound water phase occurs freely like the case of exchanging in an individual microfibril surface (Figure 8a). With increasing temperature, the amount of bound water in the above enclosed space become larger despite of increasing the activity of free water, resulting in suppressing increase in T_2.

Evaluation for Amount of Bound Water

Average particle size of cellulose in TCG, which nearly corresponds to a length of individual microfibril (see Figure 1b), was 0.16 μm by a laser-scattering method.[17] This value is one-order smaller than 4.0–8.2 μm estimated for MCC suspension.[5] Since the amount of bound water reflects the surface area of cellulose, it is expected that the amount of bound water in TCG is greatly lager than that in MCC suspension because of smaller particle size. To verify this quantitatively, estimation of amount of bound water was carried out for TCG using the method proposed previously.[5] The relative amount of bound water, α was evaluated at 25 °C from the relationship between cellulose content and T_2 of water for TCG.[5,15] α is de-

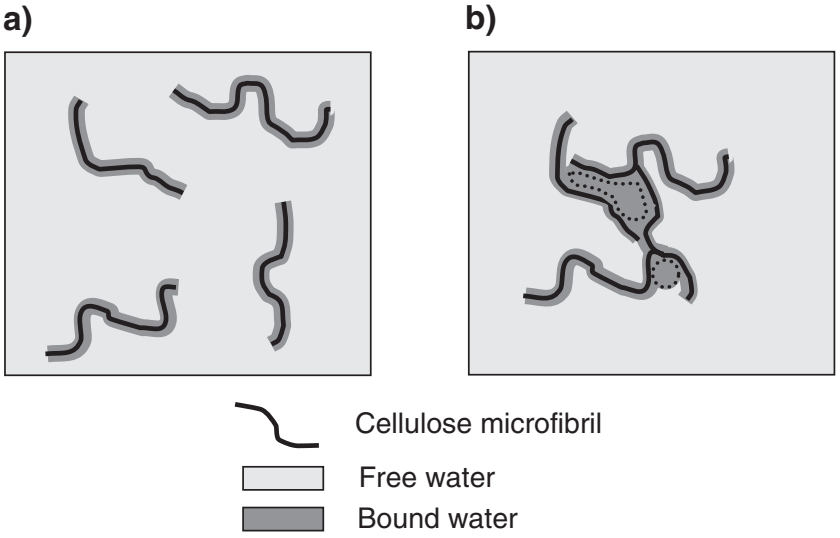

Figure 8. Model illustration of particle dispersion state and distribution of bound water in TCG gel sample: (a) Bound water is distributed vicinity of microfibril surface at a low temperature, due to low aggregation, (b) With increase in contacting probability between microfibrils at higher temperatures owing to increase in molecular mobility of free water, the new space (area surrounded by dotted line) accommodating bound water is created among the loose aggregates by microfibrils (capillary effect[16]).

fined as ratio of f_b againt f_c (eq 2), where f_b and f_c mean proton mole fractions of bound water and cellulose against whole protons in suspension, respectively.

$$\alpha = \frac{f_b}{f_c} \tag{2}$$

According to our previous work, T_2 ($T_{2,obs}$) of water observed at 25 °C for cellulose suspension may be described by eq. 3 or 4 as function of f_c.

$$\frac{1-f_c}{T_{2,obs}} = \frac{f_b}{T_{2,b}} + \frac{1-f_b-f_c}{T_{2,f}} \tag{3}$$

$$T_{2,obs} = \frac{(1-f_c)T_{2,f}T_{2,b}}{T_{2,b} + (\alpha T_{2,f} - \alpha T_{2,b} - T_{2,b})f_c} \tag{4}$$

where $T_{2,f}$ and $T_{2,b}$ are T_2 of free water and bound water. Both were assumed to show no dependence of cellulose content in the observed system. We used $T_{2,f} = 3.0\,s$ and $T_{2,b} = 5 \times 10^{-3}\,s$ corresponding to T_2 of deionized water at 25 °C and the value evaluated for MCC aqueous suspension system.[5]

Figure 9 shows the T_2 *vs.* f_c for TCG samples at 25 °C and at pH = 3.5 ± 0.1. In the figure, fitting curve using eq. 4 is shown as a solid line. Good fitting by eq. 4 was obtained also in the present system. α obtained by fitting was 5.55, being much larger than that evaluated for MCC suspensions (1.39–1.83). This suggests that amount of bound water for TCG is larger than that for MCC suspensions. In other words, surface area per unit weight of TCG is larger than that of MCC.

Average particle size of MCC suspensions lies between 4.0–8.2 μm and that of TCG suspension is *ca.*

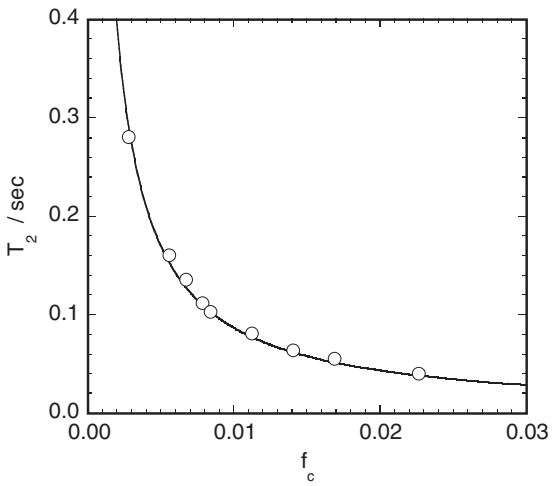

Figure 9. Relation between T_2 of water observed for several TCG samples and molar fraction of protons in cellulose (f_c) and a fitting curve (solid line) optimized according to eq 4.

0.16 μm. The ratios of average particle size (MCC/TCG) lies in the range 25–51, and the ratios of surface area per unit weight (MCC/TCG) are given in the range of 0.004–0.0016 by the simple spherical assumption. This value is much smaller than the α ratio (MCC/TCG = 0.25–0.33). The reason is explained as follows: Judging from the similar results[2] on particle size for TCG by AFM observation and a laser scattering method, the particles constituting TCG is downsized to nanofibers due to the severe acid-hydrolysis procedure applied in its production in the dispersion state. In contrast, MCC is produced by relatively mild acid-hydrolysis and therefore particle size is much

larger than those of TCG. However, as shown in the previous study for MCC powder,[8] particles constituting MCC are strong aggregates of rod-like microfibrils 10 nm in diameter and several 100 nm in length. Average size of microfibrils of MCC has fairly same level to that of TCG. Although these microfibrils in MCC suspension are strongly aggregated owing to the production process, water molecules can freely penetrate the crevices between microfibrils, contributing to strong swelling of MCC. This is supported by the fact that MCC in suspension also is downsized to individual microfibril units by a microwave treatment, as seen in the previous work.[8]

Judging from penetration of water, the surface area of MCC should be considerably much higher than that expected from apparent size estimated by a laser-scattering method.[17] Therefore, the α ratio (MCC/TCG = 0.25–0.33) may reflect the ratio of surface area of each microfibril. Microfibrils in MCC are highly crystallized but the crystallinity of microfibrils in TCG is very low. This may influence the state of bound water on the microfibril surface such as thickness of bound water layer, leading to distinct differences between TCG and MCC.

Effect of Ionic Strength on the Viscosity of TCG

The stability of TCG is quite important in order to apply this material.

Figures 10 and 11 show the viscosity–shear rate (η–$\dot{\gamma}$) plots and the viscosity–shear stress (η–σ) plots for 0.5 wt% TCG suspension (TCG-0.5) at pH = 1.0–12.0 and at 25 °C, respectively. TCG samples below pH = 2.0 show so-called synerisis. At pH = 1.0–4.0 and 8.0–12.0, viscosity–shear stress considerably changes with slight pH change. In contrast, at pH = 5.0–7.0, all suspensions were low viscous fluids (not forming a gel) and theological data showed little pH dependence. The network in TCG is thus stable in a neutral region but sensitively changes in the lower or higher pH region.

Figure 12a–c shows pH dependence on two rheological parameters ($\eta_{\gamma=1}$ and $\eta_{\gamma=1}/\eta_{\gamma=100}$) and relative transmittance T_r at 660 nm (blank: deionized water), respectively. $\eta_{\gamma=1}$ and $\eta_{\gamma=100}$ are viscosities at $\dot{\gamma} = 1\,s^{-1}$ and $100\,s^{-1}$, respectively. $\eta_{\gamma=1}/\eta_{\gamma=100}$ was used as an index of thixotropic nature of each suspension. $\eta_{\gamma=1}$ and $\eta_{\gamma=1}/\eta_{\gamma=100}$ abruptly increase with change of pH from neutral region (pH = *ca.* 5–9) to the acid side or alkaline side, but decrease drastically in the further low pH (<3) and high pH (>11) regions. Transparency was kept constant in a wider pH range (*ca.* 4–11) than rheological parameters, but abruptly decreased at acidic and alkaline.

pH Dependence in Figure 12a–c is interpreted as below: In the case where microfibrils are dispersed independently or associated loosely to form microgel with relatively small size, the viscosity of the TCG suspension should be low because of the loss of three dimensional network (this state is referred to as State A). If an additional attractive force between microfibrils is applied to State A, microfibrils interact with each other preferably to form an expanding network (State B). The viscosity of TCG suspension increases in State B, as discussed for MCC/water suspension in the previous paper.[5] In the case of TCG-0.5, the network in State B results in gel state with no fluidity irrespective of low cellulose concentration. If further attractive forces between microfibrils work well, aggregation of the network domain becomes to occur (State C). In such state, individual aggregates function

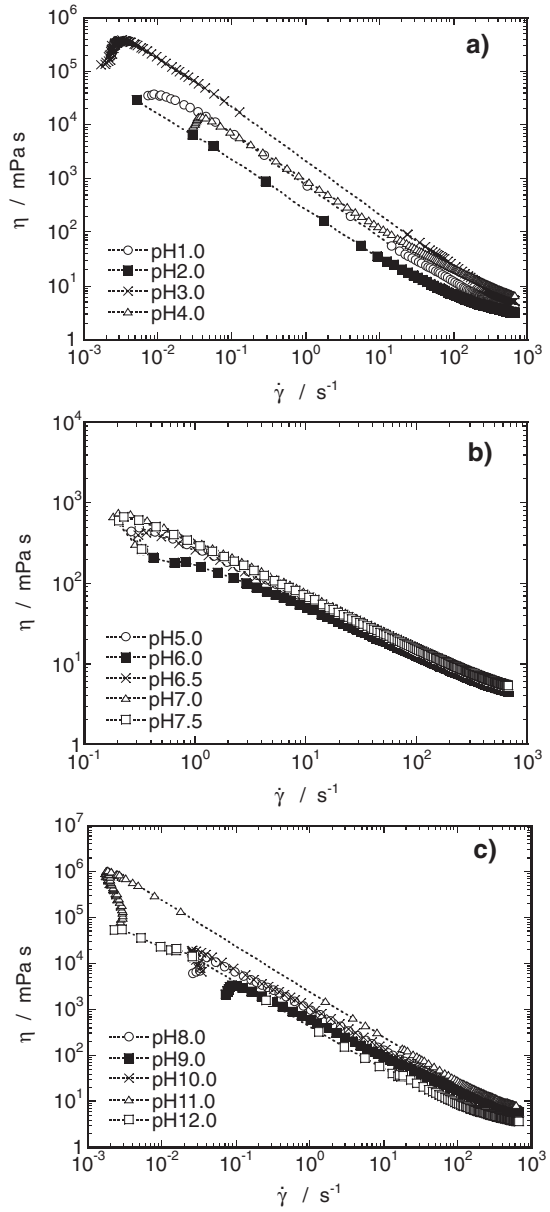

Figure 10. Viscosity (η) *vs.* shear rate ($\dot{\gamma}$) plot for TCG-0.5 at 25 °C in (a) acidic, (b) neutral region, and (c) alkaline regions.

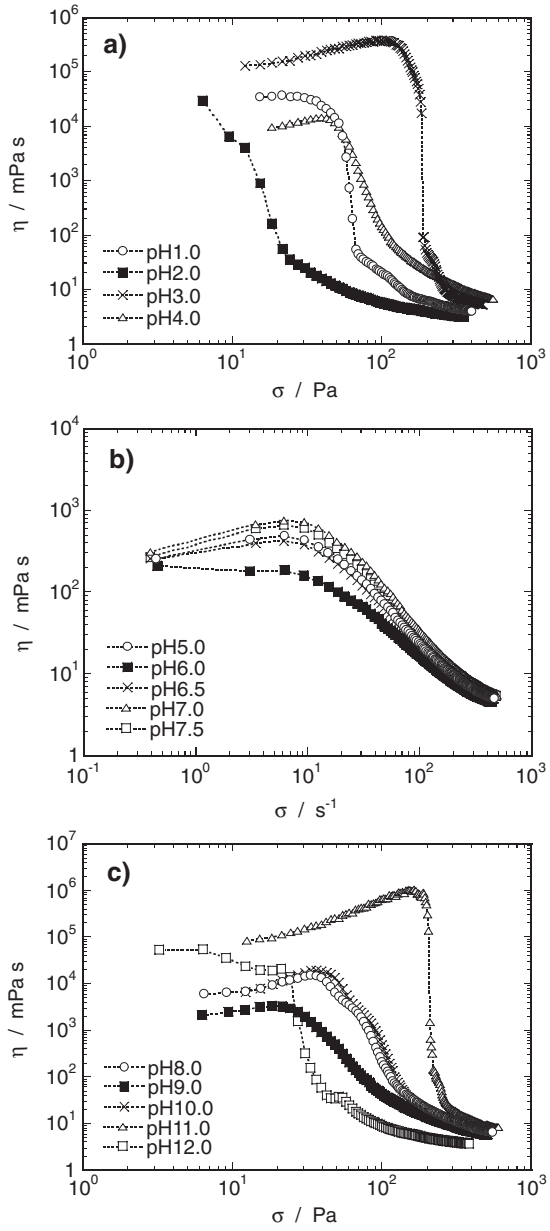

Figure 11. Viscosity (η) *vs.* shear stress (σ) plot for TCG-0.5 at 25 °C in (a) acidic, (b) neutral region, and (c) alkaline regions.

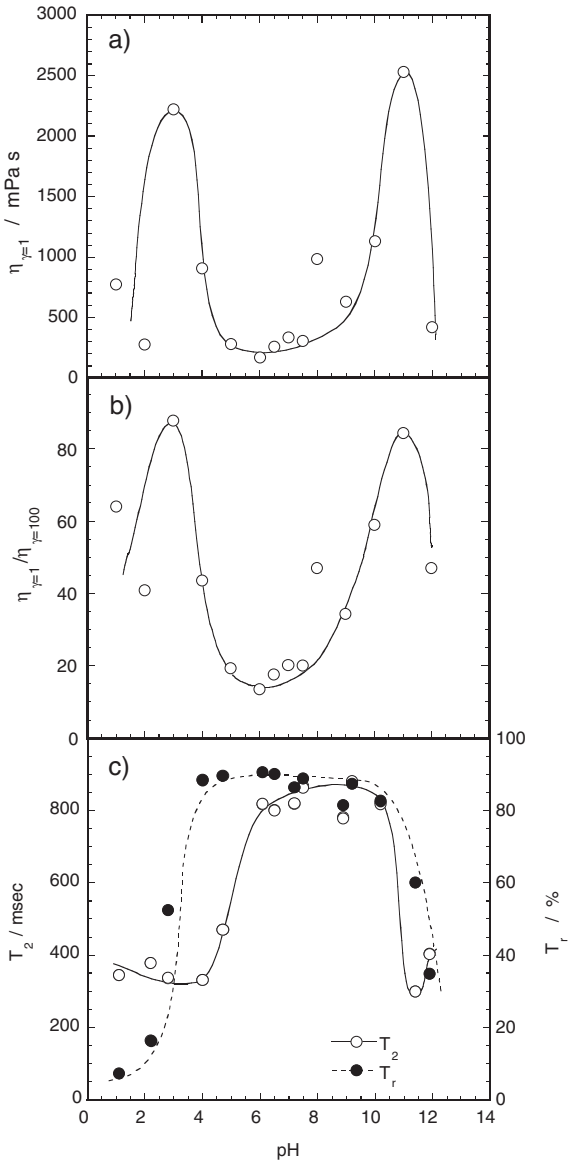

Figure 12. pH Dependence of $\eta_{\dot{\gamma}=1}$ (a), $\eta_{\dot{\gamma}=1}/\eta_{\dot{\gamma}=100}$ (b), T_r and T_2 of water (c), estimated for TCG-0.5 at 25 °C: $\eta_{\gamma=1}$ and $\eta_{\gamma=100}$ mean the viscosity at shear rate $\dot{\gamma} = 1$ and 100 s^{-1}, respectively. T_r is the relative transmittance against deionized water at 660 nm.

as single solid-like particles. The viscosity becomes drastically lower because the suspension is now a dispersion of solid-like new particles with a larger particle size. Images of States A–C are illustrated in Figure 13 which represents the relationship between viscosity and NaCl concentration for TCG-1.0.

Transparency is influenced by a light scattering at the interface between different components with different refractive indexes (microfibril, microgel and water, in this case). The difference of the refractive indexes between the inside of the network domain and the surrounding water in State B is small in comparison with that between the tightly aggregated particles and the water phase in State C. The sizes of tightly aggregated particles obviously exceed the a wavelength of visible light (0.38–0.78 μm), resulting in opacity of the suspension owing to the diffused reflection.

We consider the relationship of pH and working force between microfibrils. Since many OH groups exist on surface of cellulose microfibrils in TCG suspension, microfibrils preferably aggregate by a surface–surface interaction by a hydrogen bonding if they have no repulsive force mutually. The stability of TCG intimately is related to the fact that cellulose has a characteristic negative charge on surface. The reason why the surface of cellulose solid has negative charge despite of electrical neutrality of cellulose chain, is not understood like the case of the aqueous colloids of nanoparticles such as SiO_2 and TiO_2. Neg-

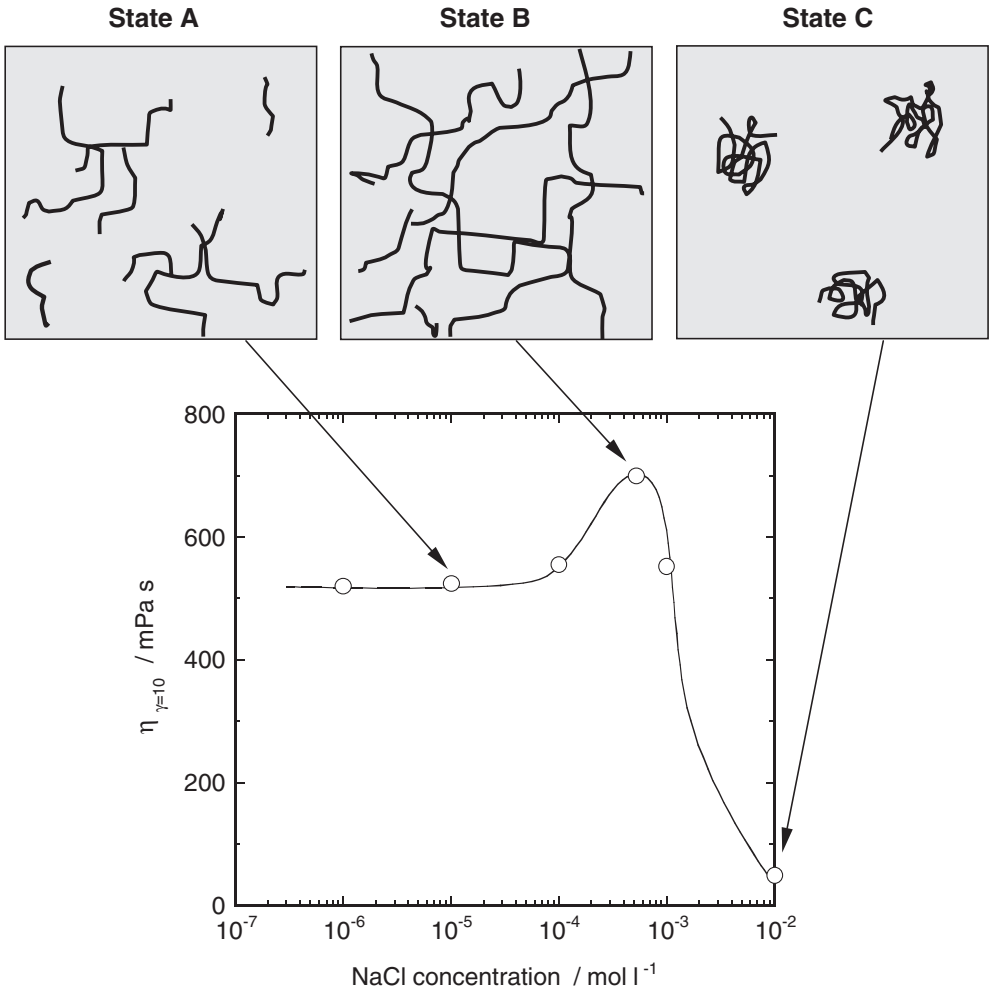

Figure 13. Dependence of T_r and $\eta_{\gamma=10}$ for TCG-1.0 on NaCl concentration in the system and schematic models of dispersion state (States A–C) in TCG at the NaCl concentration regions.

ative charge on cellulose surface is probably not due to an existence of heterogroups having negative charge (*e.g.*, carboxyl group and sulfuric group). This is also supported by the fact that conventional cellulose shows ζ potential within the range of -30 ± 10 mV[9] with no relation to structural factors such as degree of polymerization (density of chain end groups) and production history (trace amount of hetero groups derived from a partial sub-reaction). Negative charge of cellulose surface may be related to polarization state of multiple OH groups on surface and water molecules around them.

TCG suspensions in neutral pH region have a certain amount of positive ions (H^+ and a trace of positive ions as impurities such as Na^+, Ca^{2+} and NH_4^+) make a weakly positive layer around microfibril surface as a result of electrostatic interaction. TCG should be, especially in neutral pH region, stabilized by this positive–positive repulsion in relation to the outer positive layer of microfibril.

The driving force of the outer positive layer is explained by DLVO theory[10,11] in which increase in ionic strength in aqueous phase facilitates the gradual compressing of positive outer layer on the surface of microfibrils (electric double layer). If the quantity of positive charge supplied from aqueous phase (ionic strength) becomes equal to the electrical potential of cellulose surface (isoelectric point), self-aggregation proceeds as a result of losing an electrical-repulsive force. The addition of acid or base reagent can be explained as an effect of increase in ionic strength of the system. Ionic strength is, therefore, a significant factor of the isoelectric point of the system where abrupt aggregation occurs.[18] In fact, three profiles in Figure 12a–12c for the rheological parameters and transparency are almost symmetrical about pH = 7 and the intervals of pH from neutral pH (7) to pH showing peak top in acid region and in base region are nearly equal.

Figure 12c shows the pH dependence of T_2. Note that T_2 of waters with pH = 2.0 (adding HCl), 6.7 (deionized water) and 12.0 (adding NaOH) are 2.8 s, 3.0 s and 2.9 s, respectively, almost independent of pH. In contrast, T_2 in Figure 12c shows strong pH dependence. pH regions showing the drastic change in T_2

vs. pH (Figure 12c) are nearly agree with those in $\eta_{\gamma=1}$ *vs.* pH (12a) and $\eta_{\gamma=1}/\eta_{\gamma=100}$ *vs.* pH (12b) rather than the T_r *vs.* pH (12c). Shorter T_2 (less than half of T_2 at neutral region) was observed at low or high pH region where aggregation of microfibrils proceeds. In this system, shorter T_2 for water corresponds to increase in bound water content due to the network forming by microfibrils as discussed already. In addition, a symmetrical profile about pH = 7 is seen in T_r *vs.* pH, but not in T_2 *vs.* pH. pH regions showing drastic decrease in T_2 are pH = 4–6 in acid region and pH = 10–11 in base region. This means that the change from a network formation to an aggregation with pH change more sensitively proceeds in acid region than in base region.

If the above results are explained by the effect of ion strength, the tendency similar to the pH dependences in Figure 12a–c is expected for the change of rheology by adding neutral ionic reagent such as NaCl.

Figure 13 shows NaCl concentration dependence of the viscosity ($\eta_{\gamma=10}$) for TCG-1.0 at 25 °C. Here, $\eta_{\gamma=10}$ is viscosity at $\dot{\gamma} = 10\,s^{-1}$. With increasing NaCl concentration, $\eta_{\gamma=10}$ increases by forming a network (loose aggregation). Further aggregation gives abrupt decrease of $\eta_{\gamma=10}$. In this figure, schematic models of dispersion state (corresponding to State A–State C in the discussion for pH) are shown.

Rheological changes of TCG by adding acid, base and neutral ionic reagent can be explained by the simple effect of ionic strength. T_2 analysis for water clarifies network or aggregation states of cellulose microfibrils in TCG, in relation to viscosity and transparency.

REFERENCES

1. H. Ono, *Cellulose Commun.*, **6**, 101 (1999).
2. H. Ono, Y. Shimaya, T. Hongo, and C. Yamane, *Trans. Mater. Res. Soc. Jpn.*, **26**, 569 (2001).
3. O. A. Battista, "Microcrystal Polymer Science," McGraw-Hill, New York, N.Y., 1975, p 17.
4. H. Ono and H. Amakawa, Japan Patent Application 2003-73229 (September 3, 2001).
5. H. Ono, H. Yamada, S. Matsuda, K. Okajima, T. Kawamoto, and H. Iijima, *Cellulose*, **5**, 231 (1998).
6. M. Fukuda, K. Kohada, H. Kawai, H. Tanaka, K. Fukumori, and T. Nishi, *Sen-i Gakkaishi*, **44**, 428 (1988).
7. A. Viallat and S. Perez, *J. Polym. Sci., Part B: Polym. Phys.*, **31**, 1567 (1993).
8. H. Ono, M. Inamoto, K. Okajima, and Y. Yaginuma, *Cellulose*, **4**, 57 (1997).
9. "Polymer Handbook 3rd ed.," J. Brandrup and E. H. Immergut, Ed., John Wiley & Sons, New York, N.Y., 1989, p V153.
10. B. V. Derjaguin and L. D. Landau, *Acta Physicochim. U.R.S.S.*, **14**, 633 (1941).
11. E. J. W. Verway and J. Th. G. Overbeek, "Theory of the Stability of Lyophobic Colloids," Elsevier, Amsterdam, 1948.
12. S. Meiboom and D. Gill, *Rev. Sci. Instrum.*, **29**, 688 (1958).
13. S. Onogi, "Kagakusya No Tameno Rheology," Tokyo Kagaku Dojin, Co., Ltd., Tokyo, 1982, pp 37 and 97.
14. N. Bloembergen, E. M. Purcell, and P. V. Pound, *Phys. Rev.*, **73**, 679 (1948).
15. J. R. Zimmerman and W. E. Brittin, *J. Phys. Chem.*, **61**, 1328 (1957).
16. G. Martini, *J. Colloid Interface Sci.*, **80**, 39 (1981).
17. M. Kerker, "The Scattering of Light," Academic Press, New York, N.Y., 1969, chapt. 5.
18. F. Kitahara, "Bunsan Gyosyu no Kaimei to Ouyou Gijutsu," Fuji-Techno System Co., Ltd., Tokyo, 1992, p 47.